Glass Carrier Based Packaging Approach Demonstrated on a Parallel Optoelectronic Transceiver Module for PCB Assembling

Lars Brusberg, Henning Schröder, Robert Erxleben, Ivan Ndip, Michael Töpper, Nils F. Nissen, Herbert Reichl
Fraunhofer Institute for Reliability and Microintegration,
Gustav-Meyer-Allee 25, 13355 Berlin/Germany,
lars.brusberg@izm.fraunhofer.de

Abstract

Glass as a carrier material for electrical and optical interconnects has many benefits compared to conventional materials like silicon, ceramic or polymer based laminates because of its excellent dielectric and transparent properties that are becoming important for electrical high-frequency signal wiring as well as for optical wave guiding. Furthermore, the integration potential of glass is excellent because of the dimensional stability under thermal load and the coefficient of thermal expansion matching that of silicon ICs. A small pitch size of conductor traces, small scale through-vias and high alignment accuracy are the key requirements that will be achieved from glass carrier based packaging. Another outstanding benefit is the transparency of glass that allows the planar integration of optical waveguides inside the glass core material and the light transmission through the carrier between different optical layers. This paper presents a four channel bi-directional optoelectronic transceiver module that was designed and processed using the glass carrier based packaging approach called *glassPack*. The transceiver operates with 10 Gbps per channel and has an extremely low power consumption of 592 mW. The module is mounted on a printed circuit test board and the performance is characterized by bit error rate testing.

1. Introduction

The trends of optoelectronic transceiver modules for data transmission are decreasing form factor and increasing data rate. For these issues, optoelectronic multi-channel transmitters and receivers have to be implemented in a package that can be mounted on a printed circuit board (PCB) for optical boards. State-of-the-art are multi-mode transceiver modules using a silicon, ceramic or polymer core material as carrier for optoelectronic devices like photo detectors (PD) and vertical cavity surface emitting lasers (VCSEL) as well as laser driver and amplifier integrated circuits (IC) that are all flip-chip mounted for high integration grade. The optoelectronic transceiver module targets high-speed datacom applications where electrical signals in the gigahertz frequency range have to be transformed into optical signals or vice versa for replacing electrical wires and transporting a huge amount of data over a distance on board or even beyond that. These applications need transceiver modules that are located close to the processor or memory units in a super computer or in data center servers. The presented transceiver module is made of a 500 micron thick Schott BOROFLOAT®33 carrier with electrical pads for board mounting located on the bottom side. Hermetically sealed (NEC/Schott HermeS™ [1]) tungsten plugs inside the glass electrically connect the bottom side with the electrical traces and assembled components on the top side of the glass carrier. A four channel VCSEL array and a compatible driver IC make up the transmitter part of the module. Furthermore, a four channel photo detector (PD) and a transimpedance amplifier (TIA) are the receiver part. All components are flip-chip mounted on the top side of the glass carrier. The light beams of the assembled VCSEL array illuminate through the transparent substrate and couple light over a mirror into a waveguide layer below, which is optically interconnected to a ribbon fiber array over a mechanical transfer (MT)-connector. The glass based module is mounted and electrically connected to a PCB.

We already demonstrated a glass based optical sensor with integrated Mach-Zehnder interferometer (MZI) waveguide structure, a fluidic channel, optoelectronic components and silicon dies [2, 3]. Also, the integration of embedded optical waveguide layers into organic laminates has been presented for electro-optical circuit board (EOCB) applications [4]. The planar integration of the optical waveguide array below the surface of the thin glass foil is done by ion-exchange technology. The resulting multimode waveguides have been characterized showing a graded refractive index profile and a propagation loss of less than 0.1 dB/cm at a wavelength of 850 nm. Glass based optical coupling elements for out-of-plane coupling manufactured by micro-polishing of the end-face show a coupling performance of 1.1dB [5]. Experiments on through-glass vias and multilayer stacking were presented for using glass as a substrate material for high density electrical interconnects [6]. A comprehensive discussion on glass based System-in-Package (SiP) technologies is published in [7].

This paper presents the design, processing and characterization of a 4 x 10 Gbps transceiver module based on glass packaging technology. In Section 2, the high-frequency simulation is introduced to evaluate the electrical performance of the tungsten through-glass-via (TGV) having a diameter of 100 microns and to design the electrical wiring on the surface sides of the glass carrier. Also in Section 2, the optical link is designed starting from the laser which propagates through the glass carrier, the 45 degree beam deflection and the light coupling into the multi-mode waveguides as well as the fiber coupling and vice versa the link to the detector. In Section 3, the module packaging process is described done on 4 inch HermeS wafers using thin film technology and thermo-compression (TC) bonding for component assembling. The paper concludes with Section 4 where the module characterization done by bit error rate testing (BERT) is presented.

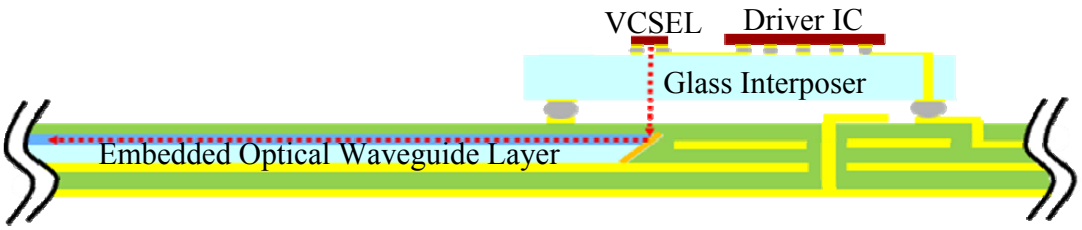

Fig. 1: System design for an electro optical circuit board (EOCB) with an embedded optical waveguide layer made of thin glass and glass based optoelectronic transceiver module. The entering electrical signal is transformed by the driver IC and the VCSEL into an optical signal which propagates over the optical path (red dotted line). On the detector side photodiode and transimpedance amplifier (TIA) IC receives and treats the optical signal and returns an electrical one.

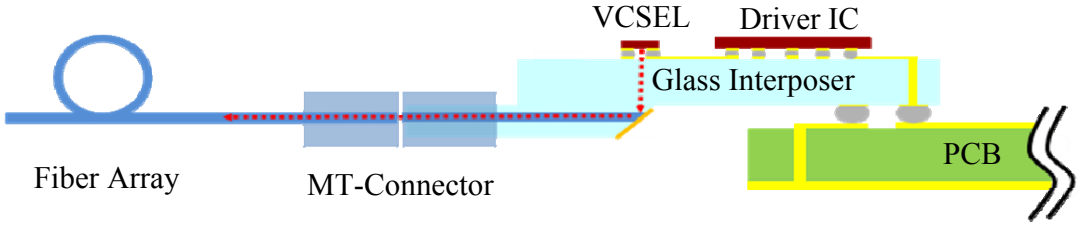

Fig. 2: Demonstrator system design for parallel optoelectronic transceiver module consists of a transmitter (VCSEL and driver) and a receiver (TIA and PD) unit, a glass interposer and optical coupling (mirror and MT-connector) to a fiber array. The drawing shows the cross Section through the transmitter part of the package. The printed circuit board (PCB) has a gap in the area below the VCSEL and the PD for the glass based optical coupling element. The beam propagation starts by the VCSEL, through the transparent glass interposer, deflected by a mirror and coupled in a waveguide which is interconnected to a fiber by a MT-connector.

2. System Design

The objective of our demonstrator is to show the capability of glass based active interposers for board level optical interconnection as shown in Figure 1. In detail, the glass carrier is the platform for electrical ICs (TIA and VCSEL driver) and electro-optical components (PD and VCSEL). In the design, the glass carrier is an interposer because of spreading the electrical connections of the ICs to a wider pitch for board mounting. State-of-the art is a parallel interconnection of different optical channels, each having data rates of at least 10Gbps [4]. An exemplary application is a server system where optical interconnects between processing units on daughter cards offer high-speed datacom links over an optical backplane.

The design of the glass based transceiver module focuses on a glass interposer which is an excellent transceiver carrier for board assembling as sketched in Figure 2. A four channel 850 nm multimode VCSEL array of U-L-M Photonics, a four channel PD array of Cosemi Technologies Inc., as well as TIA and VCSEL driver ICs of IPtronics A/S are flip-chip mounted on top of the active interposer. Instead of light coupling into the embedded optical waveguide layer as shown in Figure 1, light is coupled into a multimode fiber array using an MT-connector interface. For electrical interconnection the active interposer is mounted on a PCB. The designed module is positioned on the PCB edge as connecting unit between onboard electrical lines and the optical fibers.

2.1 Design of Transceiver Module

The transceiver module is based on a transparent through-glass interposer processed by thin film technologies. Glass substrates offer excellent dielectric properties that are becoming continuously more important for electrical high-frequency wiring and allow the simultaneous integration of optical waveguides. In Figure 3, the design of the transceiver module is presented and consists of an electrical and optical layer. During the design phase of a glass based package, the selection of a suitable glass mainly depends on reliability and process issues. For instance BOROFLOAT33 is always a good choice related to high reliability of solder joints because of excellent CTE matching to silicon dies. But some technologies only work with specific glass types because the process parameters are strictly dependent. For instance, the integration of optical functions inside the substrate using the ion-exchange technology remarkably increases the integration density but works only with high-alkaline content glasses like Schott D263™Teco. Another issue is the TGV processing. On one hand, drilling of holes in the substrate and filling those with conductive material is a possible solution. On the other hand, the HermeS approach of NEC/Schott using tungsten pins having a diameter of 100 µm that are hermetically sealed in BOROFLOAT33 glass wafers having a thickness of 500 µm is a very promising TGV solution and is used for the demonstrator package in this paper. As a result of using BOROFLOAT33, the waveguide integration into the same layer is limited. Instead, we use an optical layer below (Figure 3).

The optical layer has a planar integrated multimode waveguide array with the same optical pitch of 250 µm like the VCSEL and PD array and a mirror for 90 degree beam deflection. The electrical and optical layers are aligned to each other.

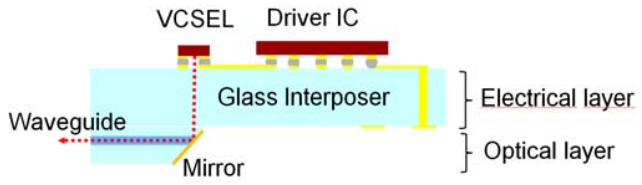

Fig. 3: Cross section drawing of the transceiver module that consists of an electrical and optical layer, which are aligned to each other. The electrical layer is a TGV interposer having thin film metalized electric circuit and assembled components on top. On the bottom side are pads for PCB interconnection. The optical layer has a planar integrated waveguide array and a mirror for 90 degree beam deflection.

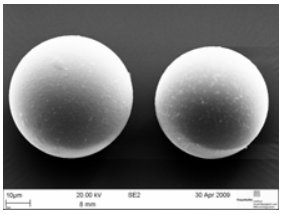

Fig. 4: A scanning electron microscope picture of two micro ball lenses.

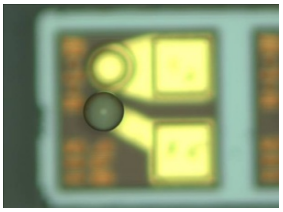

Fig. 5 A mounted micro ball lens on the active area of the VCSEL.

2.2 Optical Design

The optical transmitter and receiver interconnections were separately designed for the demonstrator. The transmitter based on the VCSEL has to couple light as much as possible into the planar waveguides of the optical layer. In general, a VCSEL is characterized by a large beam divergence. The coupling distance to the planar waveguide is 600 µm as a result of using the 500 µm HermeS for the electrical layer. The planar waveguide has an elliptical gradient index profile with 50 µm x-diameter and 100 µm y-diameter as shown in Figure 10. Ray tracing simulation was done for optimizing the coupling efficiency of the VCSEL to waveguide coupling. As a result of the 600 µm free space propagation between VCSEL and waveguide an optical systems has to be implemented for beam focusing. Because of using HermeS as electrical layer, lens integration into the interposer itself isn't an option yet. A lensed VCSEL with a small beam divergence would be a possible solution which doesn't change the thin film processing. Because of a lack of commercial available lensed VCSELs, we developed a semi-active process routine for mounting a micro ball lens on the active surface of the VCSEL. Ray tracing simulation results supported the selection of suitable micro ball lenses. We used ball lenses (Figure 4) with a diameter between 45 and 60 µm having a refractive index of 1.7. The simulation was controlled by experiments which show a divergence of 6° compared to 17° of an unlensed VCSEL. Beam divergence was measured on a beam analyzer using a laser current of 6 mA and analyzing the beam full-width (1/e²). The beam full-width (1/e²) in a distance of 600 µm is 63 µm and matches with the waveguide dimensions and the propagating modes. For demonstrator packaging lensed VCSELs were processed as shown in Figure 5.

For the receiver unit light has to be coupled out of the waveguide plane by the mirror and then free space propagated to the active area of the photodetector. The free space propagation distance is 600 µm. The circular active area has a diameter of 75 µm. The out of plane far field distribution was experimentally analyzed for the optical layer. In a distance of 600 µm most of the optical intensity covers the detector area (ø=75µm) as shown in Figure 6. As a result an optical lens system for the receiver isn't implemented in the demonstrator.

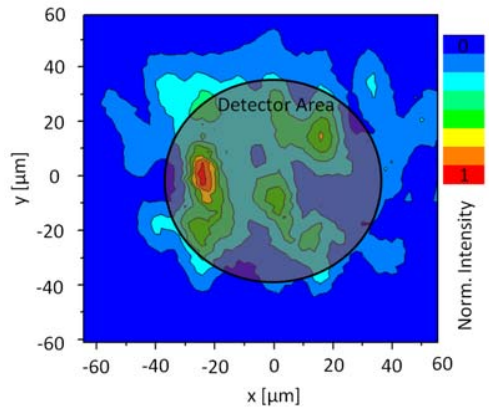

Fig. 6: Normalized intensity area scan of the multi-mode planar waveguide far-field in 600 µm distance. The detector area having a diameter of 75 µm is sketched into the plot.

2.3 Electrical Design

Planar and vertical electrical interconnects are realized using conductor traces and TGVs. As a result, much focus is placed on thin film processing for 2D interconnects on the glass surface and TGV technologies for interconnecting the front and backside of the substrate. First we studied different transmission line configurations (microstrip, stripline, coplanar and grounded coplanar) on glass by using a combination of analytic techniques and 3D full wave electromagnetic field simulations. Table 1 presents the simulation results obtained from a variation of the substrate thickness and the line thickness. Our results reveal that coplanar lines suffer the most from DC and skin effect losses but still have a transmission of 94%. We also performed simulations for TGVs by using the parameters of the HermeS approach. Simulation results of a 100 µm diameter tungsten vias in a 500 µm BOROFLOAT33 glass show that at least 87% of power is transmitted through this via at 40 GHz.

As consequence of the simulated results and process compatibility, we decided to use the HermeS wafer and a coplanar line configuration. The circuit layout of the glass interposer has to connect the ICs to the PCB for signal, control and power supply as well as to interconnect the

photodiode and VCSEL by single-ended lines to the ICs. The final circuit layout on the interposer's top side is shown in Figure 7. The lines from the ICs are spread over the glass carrier surface area and then interconnected by the through-vias to the bottom side.

Table 1: Simulation results showing transmission coefficient of different line configurations on a BOROFLOAT33 glass at 40GHz. The transmission line has a length of 5mm, is made of gold and has a characteristic impedance of 50 Ohm.

Glass Thickness [µm]	Line Thickness [µm]	Transmission coefficient of Microstrip Line [%]	Transmission Coefficient of Coplanar Line [%]	Transmission Coefficient of Grounded Coplanar Line [%]	Transmission Coefficient of Stripline [%]
100	**1**	97,5	94,6	93,5	91,6
500	**1**	99,2	93,7	93,8	97,8
500	**1**	99,2	93,7	93,8	97,8
500	**10**	99,3	94,6	94,5	98

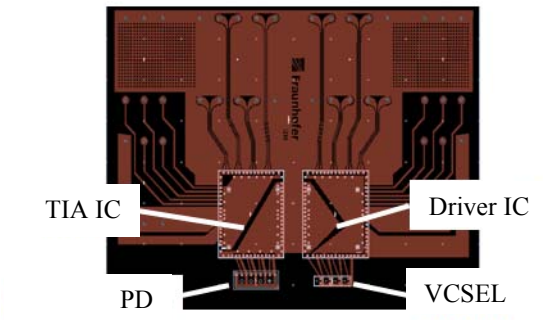

Fig. 7: Electric circuit layout on the interposer's top side. In white is depicted the footprint of the ICs, the PD array and the VCSEL array.

3. Packaging Process

The packaging process for this work was modified in contrast to a real manufacturing process because of testing issues. First the electrical layer was processed by performing thin film processing on HermeS 4 inch wafers. Then the wafer was diced. The ICs and optoelectronic components were stud bumped and thermal compressive (TC) bonded on the glass interposer. For testing purposes, the electrical circuit on the glass interposer was bonded by anisotropic conductive adhesive (ACA) onto the test board. In a parallel process, the optical layer was processed by ion-exchange waveguide integration and micro-polishing of the optical mirror. The MT-connector was attached and the optical layer actively aligned and adhesively bonded below the electrical layer.

3.1 Thin Film Process

The adhesion on glass especially by using chrome as an adhesion promoter is well known. By adapting complementary metal oxide semiconductor (CMOS) thin film processing, we have seen no difference between processing a glass or silicon wafer. We compared chrome and titanium-tungsten as adhesion promoter. Chrome provides an insignificantly better performance. As a result we sputtered a thin layer of titanium-tungsten in a combination with Au as a seed-layer for plating. Then, a 10 µm thick gold layer was plated after lithographic mask processing. After front side processing, the back side of the wafer was processed in the same way. Finally the wafers were diced and the resulting interposer has an edge length of 10 mm as shown in Figure 8.

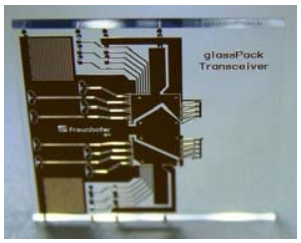

Fig. 8: Glass interposer after finishing thin film process having an edge length of 10 mm.

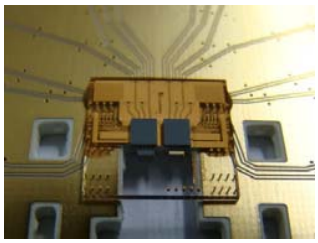

Fig. 9: Glass interposer on test board after finishing assembling process.

3.2 Assembling Process

ICs and optoelectronic components were assembled on the processed interposer by stud bumping and TC bonding to reduce the processing steps for the demonstrator and the compatibility to the gold pads of the optoelectronic components and the aluminum pads of the ICs. The bonding was done at a temperature of 250°C. Next, the assembled glass interposer was mounted by ACA bonding on the test board having a copper metallization with a flash gold layer on top. The mounted glass interposer on the test board is depicted in Figure 9.

3.3 Waveguide and Mirror Process

The waveguide processing consists of a two step processing. The first process step is performed in a molten salt mixture of sodium and silver nitrate at a temperature of 350°C. A structured alloy mask deposited on the surface of the glass foil (diffusion mask) supports the locally confined diffusion process between the glass and the salt melt. Silver ions of the salt melt diffuse into the glass and exchange takes place with sodium ions in the glass. As a result of differences in electric polarizability and ionic radii between the exchanged ions, the refractive index increases [8, 9]. The subsequent thermal ion-exchange in pure sodium nitrate buries silver ions near the surface as a consequence of reverse diffusion behavior. The index profile of the waveguide can be adjusted by process parameters such as temperature and process time. The resulting index profile of the processed multimode waveguide is shown in Figure 10. The waveguides have a propagation loss of less than 0.1 dB/cm for a wavelength of 850 nm. The cross section of such a waveguide array is depicted in Figure 11.

After the waveguide processing, a modified fiber polishing machine with a specially constructed mounting for thin glass probes is used for high-quality end-face polishing. The polishing procedure works by using polishing paper

having different grain size until the end-face has optical quality. After polishing, the surface roughness of the mirror was measured using an atomic force microscope (AFM) and the arithmetic average (R_a) is 15 nm. In Figure 12 a SEM picture shows the excellent surface quality of the mirror.

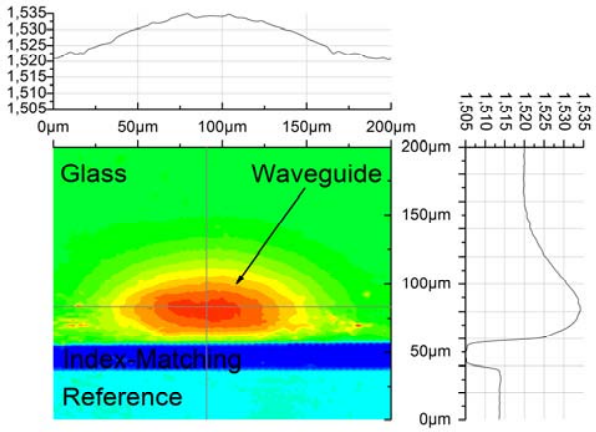

Fig. 10: Measured refractive index profile of a planar integrated waveguide in Schott D263™Teco thin glass. The index maximum of 1.535 is 25µm below the glass surface.

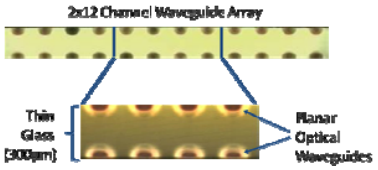

Fig. 11: Cross section of a 300µm thin glass sheet having a planar integrated 2x12 channel waveguide array processed by a two step thermal ion-exchange technology.

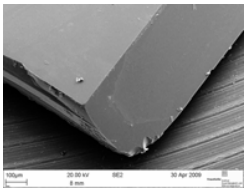

Fig. 12: SEM picture of the coupling element that shows the micro-polished mirror.

3.4 Optical Alignment Process

The light of the assembled VCSEL array illuminates through the transparent substrate and couples as a result of 90 degree beam deflection of the mirror into the waveguide array. The optical layer has to be actively aligned for a maximum of light coupling into the waveguides. We have manufactured an MT-connector for board attachment for a stable coupling efficiency between the waveguide and the fiber arrays. The optical layer and the electrical layer were actively aligned by a highly accurate micropositioning system and fixed by UV curing adhesive. A picture of this process is shown in Figure 13. The resulting final demonstrator is depicted in Figure 14. The interconnection is optically provided over an MT fiber ribbon cable and electrically provided over the test board.

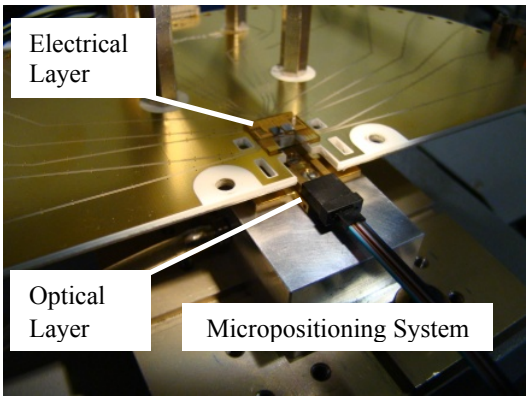

Fig. 13: Alignment process of electrical and optical layer using a highly accurate micropositioning system.

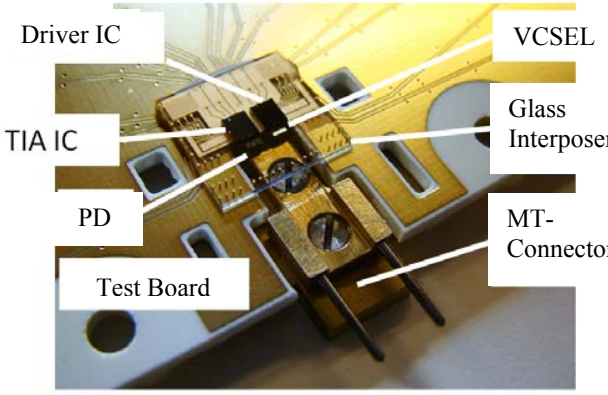

Fig. 14: Parallel optoelectronic transceiver module demonstrator mounted on a PCB.

4. Performance Characterization

For bit error rate testing, we used an Opnext XFP transceiver module which was optically interconnected by a pair of fiber to the MT-connector of our demonstrator. For electrical interconnection to signal, control and power supply the interposer was mounted on the test board by ACA bonding as described above. The bit error rate testing was performed at a data rate of 10 Gbps. The eye opening of transmitter channel one can be seen in Figure 15. Furthermore, the data transfer of all four channels of the transmitter as well as for all four channels of the receiver could be successfully performed. We characterized the conductor traces of the test board by measuring the transmission by increasing the frequency as shown in Figure 16. The attenuation increases at higher frequencies. Also, the bonding interface between glass interposer and test board wasn't optimized for the demonstrator process. Due to these facts, the limited eye opening mostly results from the test board performance and the ACA bonding interface.

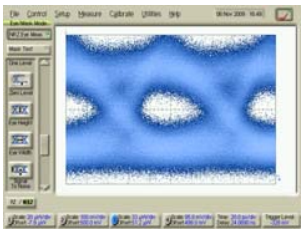

Fig. 15: Eye analysis of transmitter channel 1 at a data rate of 10 Gbps.

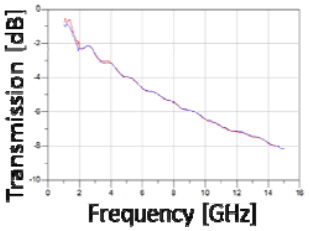

Fig. *16: Transmission measurement result of the conductor lines on the PCB with shows an attenuation increase at higher frequencies.*

The ICs were operated with 3.3 V supply and medium range control settings (bias and modulation current) and without emphasis. Under these conditions the power consumption was 86 mW per channel for the receiver and 62 mW per channel for the transmitter.

During operation in our lab we monitored the thermal hot spots of the transceiver using a thermal infrared camera. The highest temperature occurs by the VCSEL array and TIA IC with a measured value of 60°C. The peak temperature is below the components threshold temperature of 85°C. Figure 17 depicts the thermal image on the top side of the interposer. Thanks to the high power efficiency of the IPtronics ICs, the demonstrator performed without a heat sink or forced convection in our lab. If the module is covered by housing, the thermal convection is much lower and thermal design is of course a hard issue using a thermally insulating carrier material like glass. Then, thermal vias have to be integrated in the interposer or forced convection has to be applied.

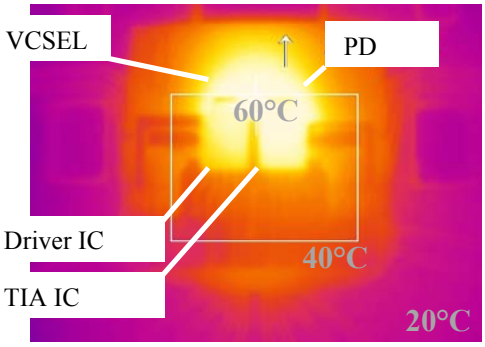

Fig. 17: Thermo monitoring of the transceiver module top side with a temperature peak of 60°C

5. Conclusion

The paper focused on process development for a glass carrier based transceiver module. The process could be performed successfully without difficulties and the final demonstrator presented. All channels of the transmitter and receiver are working. Of course the performance can be improved in a further redesign and process run. The realized demonstrator shows the excellent capability of a glass carrier based packaging approach for data and telecom applications.

Acknowledgments

The authors would like to thank all the colleagues who have supported this work. Special thanks go to O. Bochow-Neß, S. Benecke, N. Schlepple, N. Arndt-Staufenbiel, G. Lang, U. Maaß, J. Haberland, B. Otto, M. Klein, K. Kutyma, O. Ehrlich, J. Röder, V. Glaw, K. Kaletta and K. Orth. We also like to thank Mr. H. Yamamoto from Schott/NEC and Mr. G. Todt from Schott AG for their extraordinary support.

References

1. http://www.nec-schott.co.jp/english/hermes.html
2. Brusberg, L.; Schröder, H.; Arndt-Staufenbiel, N.; Wiemer, M.: “glassPack: A novel photonic packaging and integration technology using thin glass foils,” Photonics Europe, Proc. of SPIE, Vol. 6992 (2008).
3. Brusberg, L; Schröder, H.; Töpper, M.; Arndt-Staufenbiel, N.; Röder, J.; Lutz, M.; Reichl, H.: Thin Glass Based Packaging Technologies for Optoelectronic Modules "glassPack – Photonic Packaging using thin glass foils for Electrical-Optical Circuit Boards (EOCB) and sensor modules,” Proc. of ECTC, San Diego, May 26-29, 2009.
4. Schröder, H. et al "Thin Glass Based Electrical-Optical Circuit Boards (EOCB) Using Ion-Exchange Technology for Graded-Index Multimode Waveguides" Proc. 59th Electronic Components and Technology Conf, Lake Buena Vista, FL, May 2008, pp. 268-275.
5. Schröder, H; Arndt-Staufenbiel, N; Brusberg, L; Tekin, T.: “Optical coupling using thin glass based arrayed waveguide components”. Proc. of MOC, Brussels, 25-27 September 2008, pp. 56-57
6. Cui, X. et al "Glass as a Substrate for High Density Electrical Interconnect" Proc. of 10th Electronics Packaging Technology Conf, Singapore, Dec. 2008, pp. 12-17.
7. Brusberg, L; Schröder, H.; Töpper, M.; Reichl, H. "Photonic System-in-Package Technologies Using Thin Glass Substrates" Proc. of 11th Electronics Packaging Technology Conf, Singapore, Dec 2009, pp. 930-935.
8. Ramaswamy, R. V. et al "Ion-exchanged glass waveguides: a review," Journal of Lightwave Technology, Vol. 6, No. 6, (1988), pp. 984-1004.
9. Ramaswamy, R. V. "Planar buried ion-exchanged glass waveguides: difffusion characteristics" Journal of Quantum Electronics, Vol. QE-22, No. 6 (1986), pp.883-892.